THE BALTIC JOURNAL
OF ROAD AND BRIDGE ENGINEERING

2011
6(2): 107–114

STRUCTURAL BEHAVIOUR OF A SKEWED INTEGRAL BRIDGE AFFECTED BY DIFFERENT PARAMETERS

Shatirah Akib[1], Moatasem M. Fayyadh[2], Ismail Othman[3]

[1, 2, 3]*Dept of Civil Engineering, University of Malaya, 50603 Kuala Lumpur, Malaysia*
E-mails: [1]*Shatirahakib@yahoo.co.uk;* [2]*moatasem.m.f@gmail.com;* [3]*Ismail5353@um.edu.my*

Abstract. This paper presents results of an investigation on the effects of different parameters on the structural behavior of a skewed integral bridge. Flow velocities affected the scour depths at the piles, and subsequently, affected the structural behavior of the bridge's substructure. Different loading locations had varying influences on the scour depth, as well as the structural behavior of the integral bridge. Laboratory tests on a scaled down hydraulic model were undertaken to simulate the structural behavior of the scoured integral bridge. The scale of the model was chosen to simulate the actual bridge dimensions, material properties, and loading. Three different velocities were accounted for, based on the actual flow velocities of the river under the bridge, and were scaled according to the model size. Two different truck locations were adopted. The main data acquired from the experiment were the displacements and strains at specific locations on the deck slab and piles. Specifically, the results of this investigation can be utilized to identify and provide accurate design parameters for the design of a skewed integral bridge. Furthermore, results can subsequently be applied in the design of a better scour protection system.

Keywords: integral bridge, scour depth, vehicle location, flow velocity, strain, deflection.

1. Introduction

There is an increasing need to replace the current stock of bridges in Malaysia, as modern bridge systems have a lower overall cost. The huge maintenance cost incurred specifically for the expansion joints and bearings of conventional bridges has been a major concern for the local state councils and authorities. The government has also acknowledged the exceptional rise in maintenance costs, and concurrent decrease in highway revenues, as well as the serious impact on future highway construction projects. Bridges that are less than 60 m in total length are more economical and cost effective if designed as integral bridges having full structural continuity and fewer expansion joints. In view of these requirements, integral bridges have become feasible alternatives and a dramatic increase has been noted in the construction of such bridges in Malaysia. However, since the use of integral bridges is still relatively new in Malaysia, design factors relating to the effects of natural hazards and local weather, as well as environmental conditions, are unavailable and have yet to be established. One of these factors is the effect of floods on integral bridges, which is of prime concern to bridge designers. Since the 1920s, the country has experienced major floods during the seasonal monsoons, causing large concentrations of surface-runoff that exceed the capacities of most rivers. States located on the east coast of Peninsular Malaysia, such as Kelantan, Terengganu, Pahang and Johor, are usually those affected worst by these massive seasonal floods. It is only since the early 1990s that flash floods have become a concern in urban areas, and this type is perceived to be the most critical of flood types. Hence, the implementation of detailed investigations on effects of floods on integral bridges is vital. The scope of this investigation is the effect of floods on skewed integral bridge; flood related problem such as scour and its effect on skewed integral bridges are specifically investigated. Fu *et al.* (2011) found that skew angle increases slightly the effects the total strain/stress due to truck load. Saber and Alaywan (2011) conducted an experiment on full-scale test of continuity diaphragms in skewed concrete bridge girders.

The objective of this study was to investigate scour behavior, the relationships between scour depth and various parameters of a skewed integral bridge, and the main channel in flooding conditions. The model that was developed consists of a single-span integral bridge, and focused on the local scour on the abutments. Previous researchers have categorized the abutment as short and long, based on the observed flow features. Kwan (1988) investigated the effect of local scour on short abutments, finding that the local scour on short abutments and piers were similar. The principle features of the flow are the down-flow

ISSN 1822-427X print / ISSN 1822-4288 online
doi: 10.3846/bjrbe.2011.15
http://www.bjrbe.vgtu.lt

Table 1. Bridge part dimensions **(labeled in Fig. 1)**

Slab	Inclined length, mm	Width, mm	Thickness, mm
	597	172	6.5
Abutment	Length, mm	Width, mm	Thickness, mm
	172	37	26.7
Piles	Depth, mm		Diameter, mm
	170		8

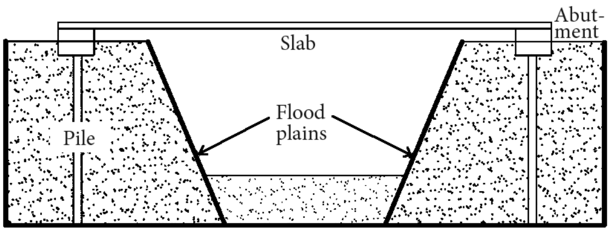

Fig. 1. Skewed integral bridge setup in the flood plains

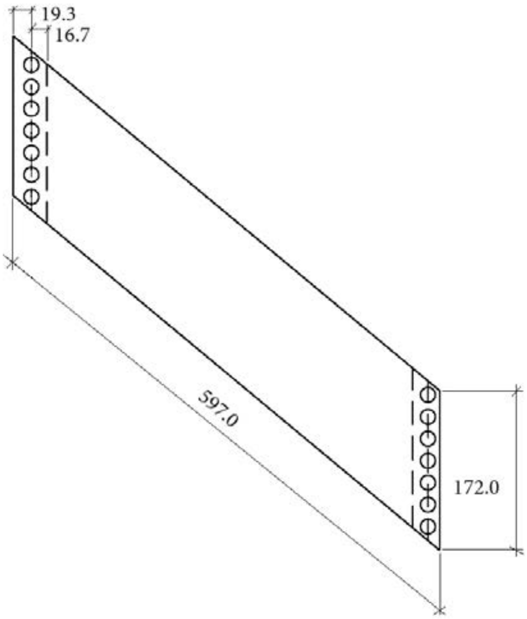

Fig. 2. Plan view of the skewed integral bridge (skew angle 56° against center line of the flood channel) (in mm)

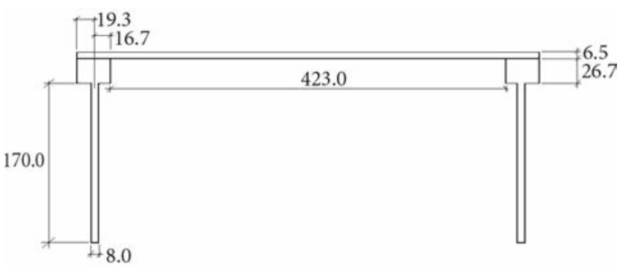

Fig. 3. Elevated view of a skewed integral bridge (in mm)

ahead of the abutments, principal vortex, and wake vortices. Many articles have been published on matters pertaining to scour on conventional bridge foundations (Breusers *et al.* 1977; Laursen 1963; Laursen, Toch 1956; Melville, Sutherland 1988; Raudkivi 1986; Shen *et al.* 1969). Kwan (1988), Lauchlan *et al.* (2001), Melville and Chiew (1999) have published local scour studies focusing on the effect of time. Scours on piers and pile groups have been well researched and documented by Kambekar and Deo (2003), Sumer *et al.* (2005), Ataie-Ashtiani and Beheshti (2006), Coleman (2005). Martin-Vide *et al.* (1998) has examined the problem related to the interaction of two widths (pier and piles) that was set at different elevations, with respect to the riverbed. The width-weighting method was recommended, because as the closer to the riverbed the base of the pier, the greater the scouring. Akib *et al.* (2009) proposed a countermeasure to reduce scour at semi-integral bridge pier by using *Epipremnum Aureum*. Scour monitoring decision framework (SMDF) was developed to help the *Minnesota Dept of Transportation* to select the most appropriate instrument given site-specific bridge and stream conditions (Lueker *et al.* 2010). Deng and Cai (2010) discussed the review of bridge scour prediction, modelling, monitoring, and countermeasures. Gogus and Dogan (2010) discovered that when the collar width was increased and it was placed at or below the bed level, the reduction in the max local scour depth increases considerably. In addition, the change of the sediment size did not affect the optimum location of the collar at the abutment, which yields the max scour reduction around the abutment.

2. Material and methods

The case study for this paper was a skewed integral bridge model. The integral bridge was built on a slab fixed into abutment, which was supported by a set of piles on both sides. Each side contained 7 circular piles embedded at the base of the flood channel. The dimensions of each part of the bridge are shown in Table 1. The model was made using perspex with a density of 1197 kg/m^3, a modulus of elasticity of 2173 kN/m^2, and Poisson's ratio of 0.39. The model was set up in the flood plain as shown in Fig. 1. Fig. 2 illustrates the plan view and the skew angle of the model. The skew angle was 56° against the center line of the flood channel. Each side of the piles was embedded into the flood plain. The elevation of the model is presented in Fig. 3. Sand was poured into the flood plain until half of the abutment was covered. The channel was also filled with 5 cm of sand in height. In order to simulate the flooding condition, the water level was set to fill on the bridge slab within the range of 8–12 mm for all of the experiments. Since the stabilization of the water level and the velocity were important in this experiment, several pre-experimental trials were conducted to ensure that specific velocity upstream and precise water level were achieved before the beginning of each experiment.

The velocities chosen for the purpose of this study include three categories: slow 0.19 m/s, medium 0.25 m/s, and fast 0.31 m/s. The riverbed material selected was uniform sand (d_{50} = 0.13 mm).

During the experiment, the changes in scour depth at both sides of the abutment and piles were recorded. The experiment was repeated three times, using the 3 different velocities (slow – 0.19 m/s, medium – 0.25 m/s, fast – 0.31 m/s). The effect of these 3 different velocities on scour depth was recorded. For the first 100 min of water flow, the scour readings were taken at 10 min intervals. Subsequent readings were recorded at an interval of 100 min, for a continuous duration of 8 h and 20 min (500 min). The last and final readings were taken the following day, after 24 h of running the experiment. After the final scour reading, a Magnetic Current Velocity Meter was used to record the velocity at different locations of the bridge model. The velocity recording was conducted after all scour readings had been taken to avoid any form of interruption to the original water flow during the scouring process.

The set of piles on each side were labeled *Q* and *P*, whereby *Q* represented the set of piles located upstream. Therefore, *Q* was the first to come into contact with the water flow and the first to be affected by it. *P* was downstream, and therefore, last to be affected by the water flow. The main data record in addition to scour depth was strain and displacement on the bridge slab and on the *Q* set of piles. The actual bridge setup during the test is shown in Fig. 4. The strain gauges (ST), and LVDTs (Linear Variable Displacement Transducer) for recording the strain displacement on the bridge slab and *Q* piles were positioned as shown in Figs 5 and 6.

The applied load contains the gravity load for the bridge weight in Y-direction (which is the vertical direction), water weight above bridge slab in Y-direction (gravity direction), uplift water pressure at the bottom of the slab in Y-direction (opposite to the gravity direction), uplift water pressure at the bottom of the abutment in Y-direction (opposite to the gravity direction), and water pressure due to flow velocity on the immersed parts of the bridge in Z-direction (the direction of the water flow).

The bridge was modeled with vehicle loading. Since it would have been rather complex to simulate vehicles moving on the bridge, the vehicle loading was modeled as

Fig. 4. Actual bridge setup during the test

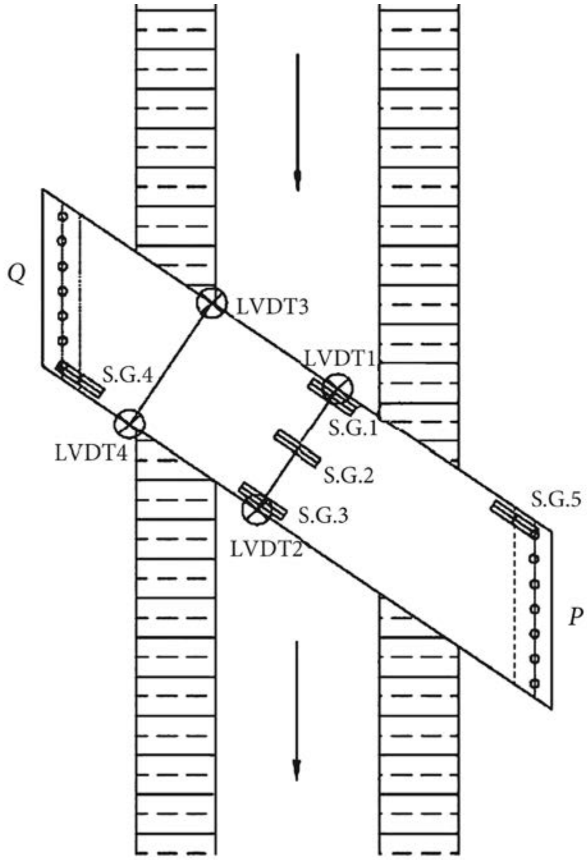

Fig. 5. Locations of STs and LVDTs on bridge slab

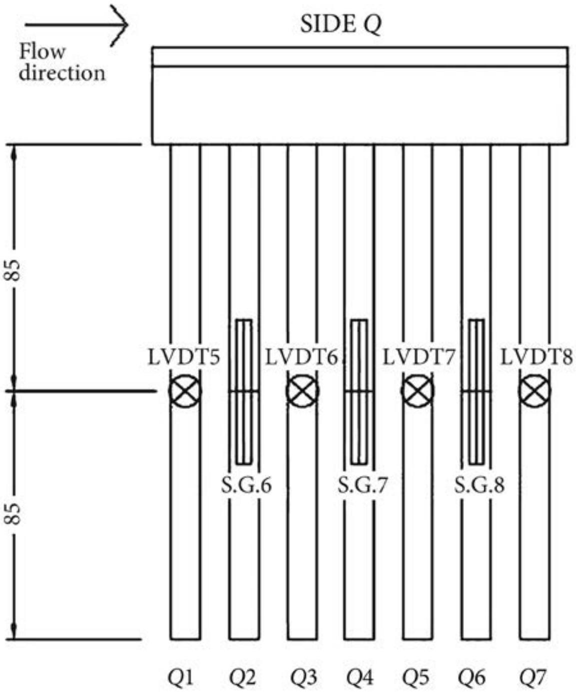

Fig. 6. Locations of STs and LVDTs on the *Q* side piles

a non-moving vehicle at both the mid-span and quarter-span of the bridge. For the purpose of this investigation, the selection of loading on the model was based on type HB loading as defined in BS 5400: Part 2 with the max 45 units of HB. One unit is equivalent to 10 kN per axle. Therefore, the load per axle is equal to number of units multiplied by unit load (45 × 10 = 450 kN), and the load per wheel is equal to the load per axle divided by 4 wheels (450/4 = 112.5 kN). In order to apply the load to the model, it was necessary to reduce the entire load to an appropriate scale. In order to compare various quantities in the prototype and model, the load ratio was derived to be equal to the shear force ratio (*SFR*).

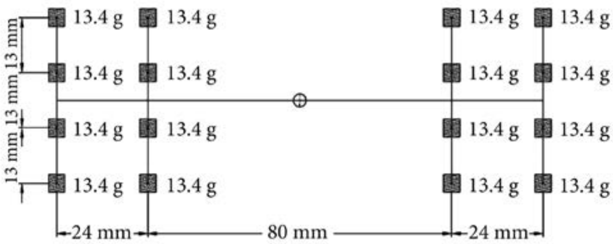

Fig. 7. Loading distribution on wheels applied on the skewed integral bridge model

$$SFR = \frac{W_p}{W_m}, \qquad (1)$$

where W_p – the weight of the prototype, kN; W_m – the weight of the model, kN.

Since the weight of the prototype was 1.028×10^6 kg, and the weight of the model was 1.1944 kg, the SFR was equal to 8.607×10^5. After applying the scale factor to the loading at each wheel, the load per wheel on the model was equal to 13.4 g. Fig. 7 shows the loading distribution applied to the wheels on the bridge model. The wheel loads were applied to the mid-span and quarter-span of the bridge slab, as shown in Figs 8, 9 respectively.

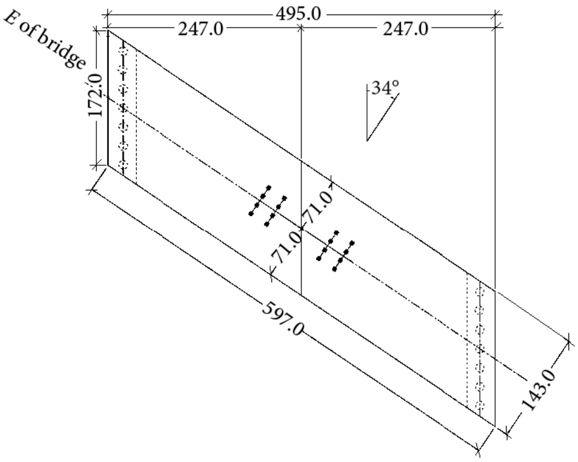

Fig. 8. Wheel loads applied at mid-span (in mm)

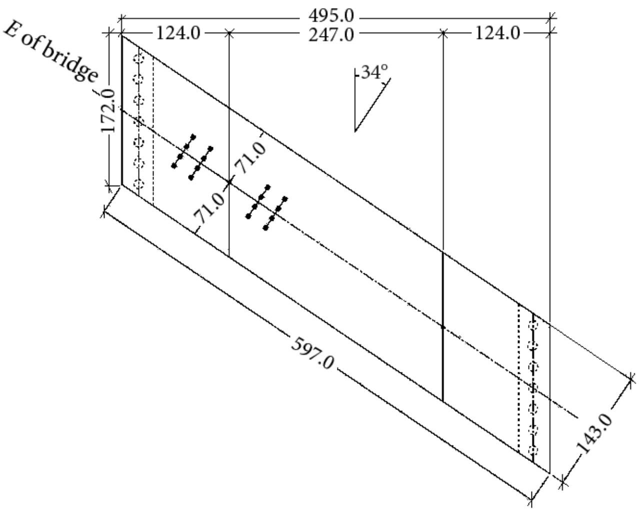

Fig. 9. Wheel loads applied at quarter-span (in mm)

3. Results and discussion

The main data resulting from the experiment were the strain and the deflection on both the bridge slab and bridge piles. The results of the scour depth at the piles with time under fast velocity were presented, and the effect of velocity location on the scour were studied, where fast flow velocity of 0.31 m/s was adopted and the reading covered the *Q* pile side. Figs 10 and 11 depict the results for the effect of the fast velocity flow on the scour depth, with the time at the pile's *Q* side with different vehicle locations.

The results demonstrated that, in the first 50 min, there was a rapid increase in scour depth, then, after 500 min, the increase slowed. After 500 min, the scour depth seemed to be constant until reaching the max scour after 24 h. When the vehicle was located at mid-span, the scour had a lower value than when it was located at quarter-span. When the vehicle was located at mid-span, the max scour occured at pile *Q*1 (93 mm), while it was 115 mm when the vehicle was located at quarter-span. Other piles had values ranging from 65 mm to 90 mm when

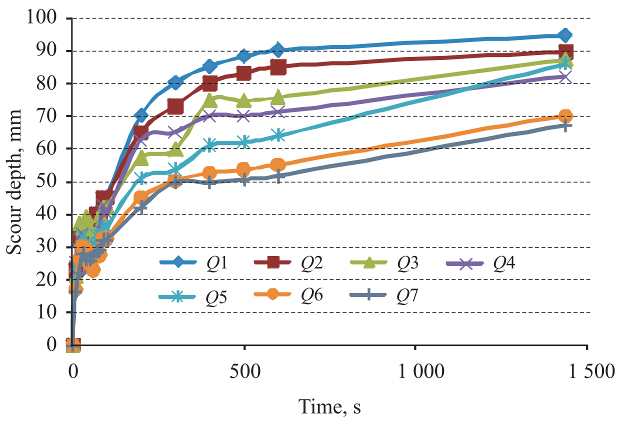

Fig. 10. The effect of fast velocity on the scour depth in *Q* side with time, vehicle located at mid-span

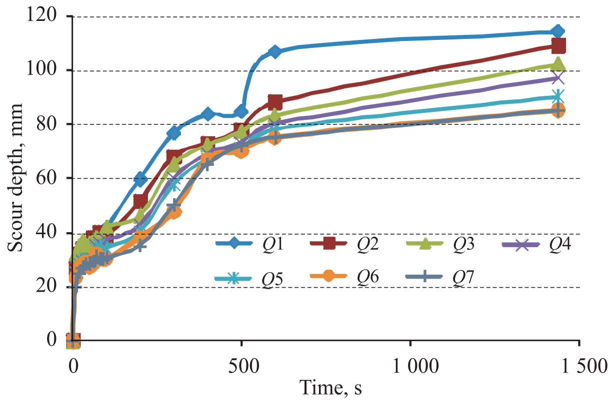

Fig. 11. The effect of fast velocity on the scour depth in Q side with time, vehicle located at quarter-span

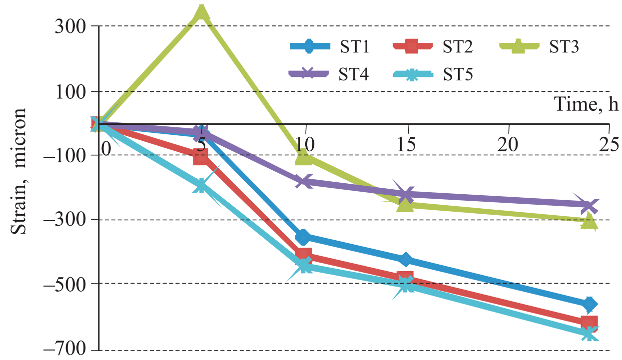

Fig. 12. Effect of scour depth on slab strain

the vehicle was located at mid-span, while iranging from 80 mm to 110 mm when the vehicle was located at quarter-span.

This results section is divided into 3 categories. The 1st category is the effect of scour depth on the structural behavior of the integral bridge. The 2nd category is the effect of flow velocity on the structural behavior of the integral bridge. The 3rd section studies the effect of vehicle location on the structural behavior of the integral bridge.

3.1. Effect of scour depth on the structural behavior

This section presents the effect of scour depth on the structural behavior of the integral bridge. The scour depth was represented by test time. During the initial time, the scour was small, and it increased with the increase of testing time until reaching the max scour at 24 h. The time intervals used were: 0 h, 5 h, 10 h, 15 h, 20 h, and 24 h. The test was done under fast velocity flow. The vehicle location adopted in this section was the mid-span. Figs 12 and 13 show the effect of scour depth with time on the strain at specific locations of the slab, as well as piles, respectively (Figs 5, 6 for STs locations).

The results indicate that the strain increased with the increase of the scour depth with time for all of the STs, and with all scour depth intervals as well, except at ST3 with scour depth at 5 h, which exhibited the reverse behavior. Figs 14 and 15 illustrate the effect of scour depth with time on the deflection of the slab and piles at specific locations (Figs 5, 6 for LVDTs locations).

The results demonstrate an increase in slab deflection until 5 h, at which time the increase rate reduced (beween 5 h and 10 h). Finally, it became constant after 10 h until reaching the max scour at 24 h. Piles deflection showed constant behavior for LVDTs No. 5 and No. 6, and increased between 0 h and 10 h. Finally, it exhibited constant bahavior after 10 h until reaching the max scour at 24 h.

3.2. Effect of flow velocity on the structural behavior

This section presents the effect of flow velocity on the structural behavior of the integral bridge. Three different velocities were adopted: slow velocity – 0.19 m/s, medium velocity – 0.24 m/s, fast velocity – 0.31 m/s. The test was

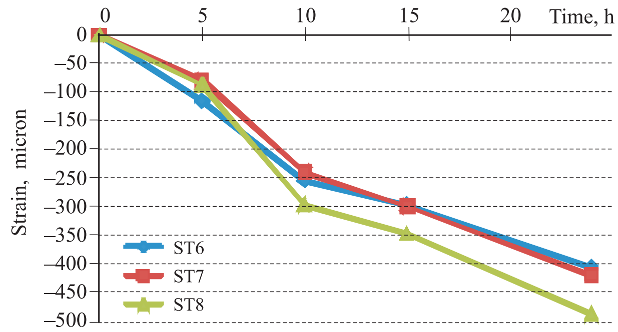

Fig. 13. Effect of scour depth on piles strain

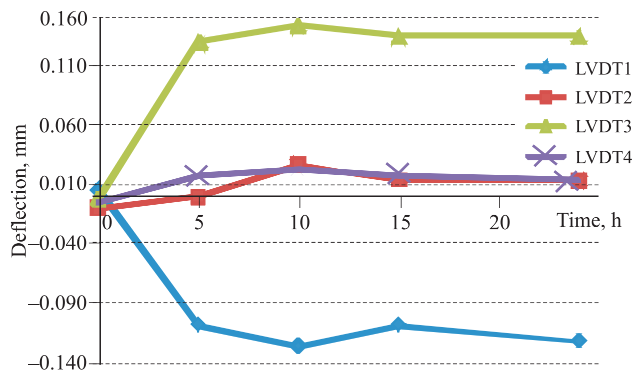

Fig. 14. Effect of scour depth on slab deflection

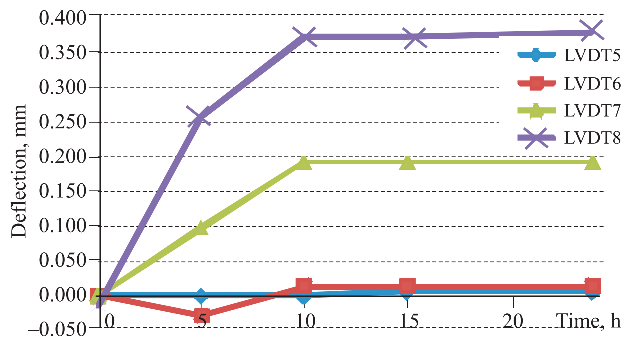

Fig. 15. Effect of scour depth on pile deflection

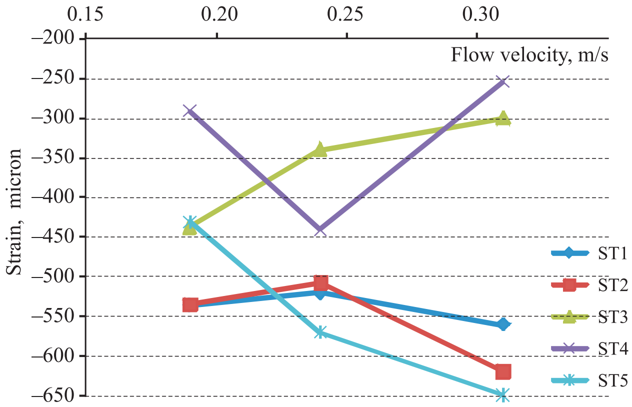

Fig. 16. Effect of flow velocity on slab strain when the load was located at mid-span

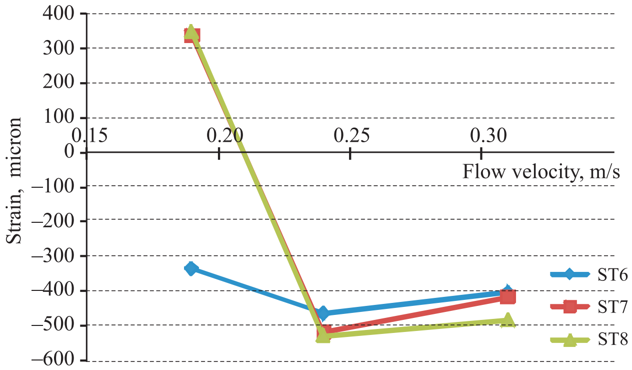

Fig. 17. Effect of flow velocity on pile strain at mid-span

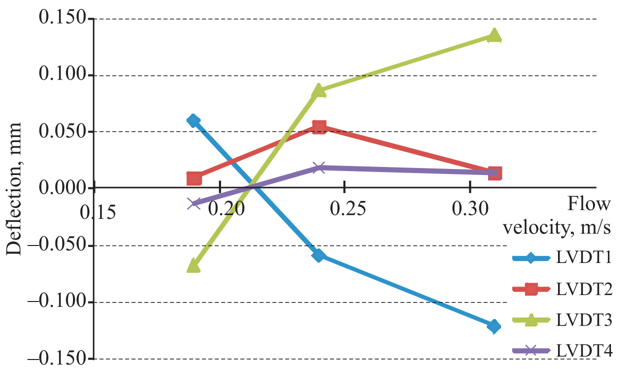

Fig. 18. Effect of flow velocity on slab deflection when the load was at mid-span

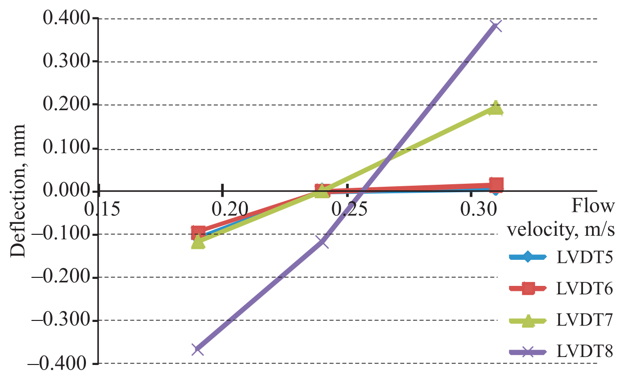

Fig. 19. Effect of flow velocity on pile deflection when the load at mid-span

conducted when the vehicle was located at the mid-span. Figs 16 and 17 present the effect of different flow velocities on the STs located on the slab and the piles.

The results of STs on the slab demonstrated that there was a difference in the effect by flow velocity with the variance of ST locations. ST1 and ST2, which were located on the forward of the centerline of the slab, showed a minor decrease when the flow velocity increased from 0.19 m/s to 0.24 m/s. They subsequently showed an incremental change when the flow velocity increased from 0.24 m/s to 0.31 m/s. This indicated that under medium velocity (0.24 m/s), there was a high effect of the uplift pressure, which balanced the downward force from the vehicle weight, water weight, and slab weight. ST3, located at the back of the centerline of the slab, decreased in strain value with the increase in flow velocity, which may be due to the fact that fast velocities resulted in a horseshoe vortex at the back side of the slab, decreasing the effect of the downward forces. The STs on the piles had decreased values for ST6 when the velocity increased from 0.19 m/s to 0.24 m/s. Then, they decreased when the velocity increased from 0.24 m/s to 0.31 m/s. ST7 and ST8 demonstrated conflicting behavior when the flow velocity increased from 0.19 m/s to 0.24 m/s, which may be explained by the increase in the horseshoe vortex of water on the sides of the piles. Figs 18 and 19 illustrate the results of the slab and pile deflection affected by different flow velocities, respectively.

The results of deflection on the slab of the integral bridge exhibited different behavior for the LVDT, located at different places on the slab. LVDT1, which was located at the forward part of the slab centerline, had an increased deflection value when flow velocity increased. This may be due to the fact that with increased flow velocity, the flow force increased on the forward part of the slab and pushed the slab down. LVDT2 showed a decrease in deflection with increased flow velocity, which may be due to the horseshoe vortex of the water at the back part of the slab, which pushed the slab upward. LVDT3 and LVDT4, which were located above the abutment on the Q piles side, exhibited a decrease in deflection with an increase of flow velocity from 0.19 m/s to 0.24 m/s. Then, they showed a slight increase in deflection when the flow velocity increased from 0.24 m/s to 0.31 m/s. This may be explained by the composite effect of the loading on the slab, where an increase of flow velocity increased the uplift pressure and the horseshoe vortex.

The results indicated a decrease in the deflection value for LVDT5 and LVDT6, and conflicting deflection values for LVDT7 and LVDT8 with the increase in flow velocity.

3.3. Effect of vehicle location on the structural behavior

This section presents the effect of vehicle location on the structural behavior of the integral bridge. Two locations were adopted, one at the mid-span and one at the quarter-span near the Q piles side. The results were based on the max scouring after a reading at 24 h. Three velocities were adopted: 0.19 m/s, 0.24 m/s, and 0.31 m/s. A total of six cases were studied, including: SM (slow flow velocity and vehicle loading at mid-span), SQ (slow flow velocity and vehicle loading at quarter-span), MM (medium flow velocity and vehicle loading at mid-span), MQ (medium flow velocity and vehicle loading at quarter-span), FM (fast flow velocity and vehicle loading located at mid-span), and FQ (fast flow velocity and vehicle loading located at quarter-span). Figs 20 and 21 depict the effect of different cases on the slab and the piles strains, respectively.

When the vehicle was located at quarter-span, it caused the decrease in the slab strain for both slow and fast velocities, while for medium velocity showed conflicted behaviour.

The results show that different vehicle locations had varying influences on the structural behavior of the integral bridge. Generally, when the vehicle was located at the quarter-span, the strain values on the piles were increased for both slow and medium velocity, while fast velocity showed conflicting behavior. Figs 22 and 23 show the results of the slab and piles deflection affected by vehicle location.

The results demonstrate that different vehicle locations had varying influnce on the slab deflection.

4. Conclusions

Research and innovation regarding the effects of different parameters on the structural behaviour of a skewed integral bridge were introduced in this study. Flow velocities affected scouring over time. Scour depth had a direct effect on the structural behavior, such as strains and displacements of the bridge substructure. Strain increased as the scour depth increased for almost all of the strain gauges (STs) and scour depth intervals. Flow velocity had a direct effect on the structural behavior of the integral bridge, due to increase of flow force. Strains and displacement on the slab and piles varied, due to location and the flow velocities. Finally, vehicle location had a different influence on the structural behavior.

References

Akib, S.; Othman, F.; Othman, I.; Sholichin, M. 2009. Semi-Integral Bridge Scour Prevention by using Epipremnum Aureum, in *Proc. of the 32nd Hydrology & Water Resources Symposium*. November 30 – December 3, Newcastle, Australia, 1217–1223.

Ataie-Ashtiani, B.; Beheshti, A. A. 2006. Experimental Investigation of Clear-Water Local Scour at Pile Groups, *Journal Hydraulic Engineering* 132(10): 1100–1104. doi:10.1061/(ASCE)0733-9429(2006)132:10(1100)

Breusers, H. N. C.; Nicollet, G.; Shen, H. W. 1977. Local Scour around Cylindrical Piers, *Journal of Hydraulic Research* 15(3): 211–252. doi:10.1080/00221687709499645

Coleman, S. E. 2005. Clearwater Local Scour at Complex Piers, *Journal Hydraulic Engineering* 131(4): 330–334. doi:10.1061/(ASCE)0733-9429(2005)131:4(330)

Deng, L.; Cai, C. S. 2010. Bridge Scour: Prediction, Modeling, Monitoring, and Countermeasures – Review, *Practice Periodical on Structural Design and Construction* 15(2): 125–134. doi:10.1061/(ASCE)SC.1943-5576.0000041

Fu, G.; Zhuang, Y.; Feng, J. 2011. Behavior of Reinforced Concrete Bridge Decks on Skewed Steel Superstructure under

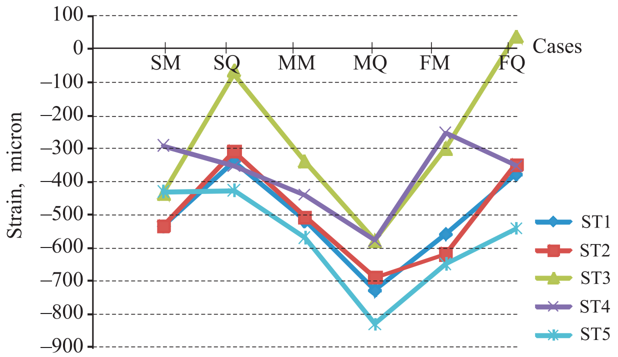

Fig. 20. Effect of vehicle location on slab strain

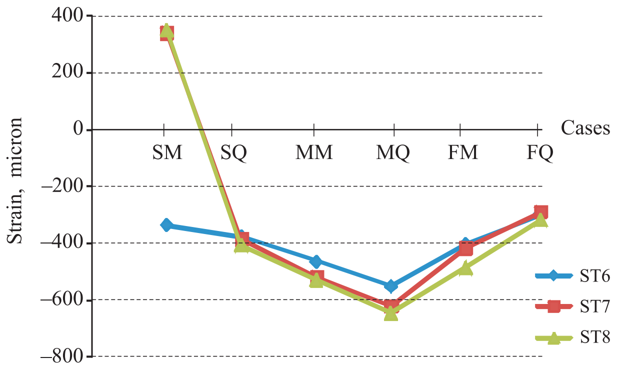

Fig. 21. Effect of vehicle location on pile strain

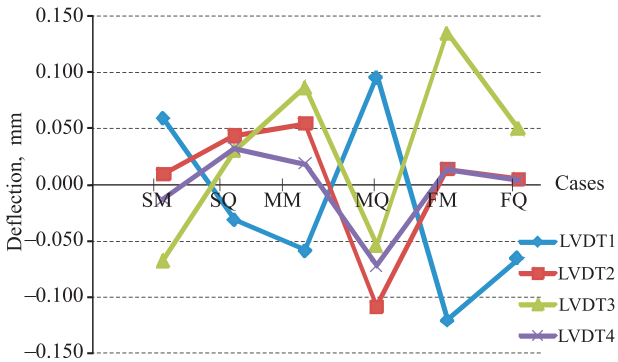

Fig. 22. Effect of vehicle location on slab deflection

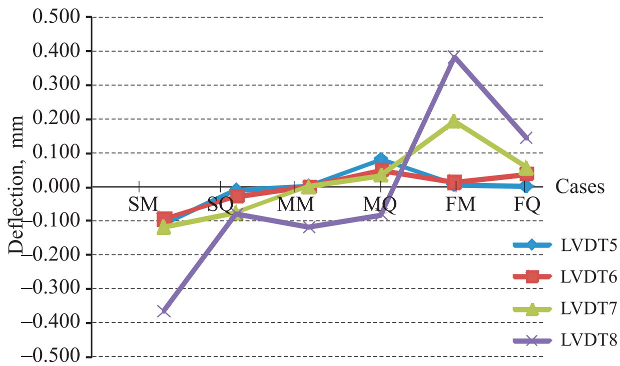

Fig. 23. Effect of vehicle location on pile deflection

Truck Wheel Loads, *Journal of Bridge Engineering* 16(2): 219–225. doi:10.1061/(ASCE)BE.1943-5592.0000142

Gogus, M.; Dogan, A. E. 2010. Effects of Collars on Scour Reduction at Bridge Abutments, in *Proc. of the* 5th *International Conference on Scour and Erosion (ICSE-5)*. November 7–10, 2010, San Francisco, CA, USA. 997–1007. doi:10.1061/41147(392)100

Kambekar, A. R.; Deo, M. C. 2003. Estimation of Pile Group Scour Using Neural Networks, *Applied Ocean Research* 25(4): 225–234. doi:10.1016/j.apor.2003.06.001

Kwan, T. F. 1988. *A Study of Abutment Scour*. Report No. 451. Auckland: The University of Auckland. 461 p.

Lauchlan, C. S.; Coleman, S. E.; Melville, B. W. 2001. Temporal Scour Development at Bridge Abutments, in *Proc. of the 29th Congress IAHR*. Beijing, China.

Laursen, E. M. 1963. Analysis of Relief Bridge Scour, *Journal of the Hydraulics Division* 92(HY3): 93–118.

Laursen, E. M.; Toch, A. 1956. *Scour Around Bridge Piers and Abutments*. Bulletin No. 4, Iowa Highways Research Board, Ames, Iowa, USA.

Lueker, M.; Marr, J.; Hendrickson, V.; Winsted, V. 2010. Bridge Scour Monitoring Technologies: Development of Evaluation and Selection Protocols for Application on River Bridges in Minnesota, in *Proc. of the* 5th *International Conference on Scour and Erosion (ICSE-5)*. November 7–10, 2010, San Francisco, CA, USA. 949–957.

Martin-Vide, J. P.; Hidalgo, C.; Bateman, A. 1998. Local Scour at Piled Bridge Foundations, *Journal of Hydraulic Engineering* 124(4): 439–444. doi:10.1061/(ASCE)0733-9429(1998)124:4(439)

Melville, B. W.; Chiew, Y. M. 1999. Time Scale for Local Scour at Bridge Piers, *Journal of Hydraulic Engineering* 125(1): 59–65. doi:10.1061/(ASCE)0733-9429(1999)125:1(59)

Melville, B. W.; Sutherland, A. J. 1988. Design Method for Local Scour at Bridge Piers, *Journal of Hydraulic Engineering* 114(10): 1210–1226. doi:10.1061/(ASCE)0733-429(1988)114:10(1210)

Raudkivi, A. J. 1986. Functional Trends of Scour at Bridge Piers, *Journal of Hydraulics Engineering* 112(1): 1–13. doi:10.1061/(ASCE)0733-9429(1986)112:1(1)

Saber, A.; Alaywan, W. 2011. Full-Scale Test of Continuity Diaphragms in Skewed Concrete Bridge Girders, *Journal of Bridge Engineering* 16(1): 21–28. doi:10.1061/(ASCE)BE.1943-5592.0000126

Shen, H. W.; Schneider, V. R.; Karaki, S. S. 1969. Local Scour Around Bridge Piers, *Journal of the Hydraulics Division* 95(6): 1919–1940.

Sumer, B. M.; Bundgaard, K.; Fredsøe, J. 2005. Global and Local Scour at Pile Groups, *International Journal of Offshore and Polar Engineering* 15(3): 204–209.

Received 23 December 2009; accepted 17 January 2011